

A Raman Study of Titanate Nanotubes

Xin-Ying Liu and Neil J. Coville*

Molecular Sciences Institute, School of Chemistry, University of the Witwatersrand, Private Bag X3, WITS, Johannesburg, 2050 South Africa.

Received 8 December 2004; accepted 14 July 2005.

ABSTRACT

The effect of the addition of NaOH or KOH on commercial Degussa Titania P25 was investigated using TEM, Raman and *in situ* Raman spectroscopy. Treatment of titania with conc. NaOH generated a tubular material corresponding to a sodium titanate. An *in situ* Raman study on the sodium titanate nanotubes as a function of temperature revealed that the titanate structure was stable up to 700°C. Raman spectra of the titanate nanotubes after acid treatment, showed that the titanate structure was retained and EDX analysis revealed only trace amounts of sodium (0.3%) left in the material. HRTEM data are also consistent with the synthesis of protonated titanate nanotubes. An *in situ* Raman study of protonated titanate nanotubes as a function of temperature showed that the material was stable up to 150°C, while anatase appeared at $T > 300^\circ\text{C}$. An *in situ* Raman study of the protonated titanate nanotubes produced from KOH as a function of temperature showed that the shape and size of the nanotubes prepared from NaOH and KOH are similar although rutile formation at 1000°C was different. A proposal for the formation of tubular titanates (and anatase) is given.

KEYWORDS

Titania nanotubes, titanate nanotubes, *in situ* Raman spectroscopy, HRTEM.

1. Introduction

The discovery of titanium oxide nanotubes has created great interest in this novel form of titania.¹ This novel high-surface material has been proposed for use as a catalyst support and it has been reported that titania nanotubes can be used as a hydrogen sensor^{2,3} or in a dye-sensitized solar cell.^{4,5}

Titanium oxide nanotubes were first synthesized in a polymer mold, on which titanium oxide was deposited electrochemically.⁶ Since this first report, a variety of different Ti containing precursors have been used to make the tubular titania materials^{7,8} including approaches using supermolecular assembly,^{9,10} sol-gel methods using a polymer fibre as template¹¹ and anodic oxidation of titanium.¹² Tubes 10 μm long and 100–200 nm in diameter have been synthesized by the above processes.

Titanium oxide nanotubes with smaller diameter and better crystallinity have also been synthesized by a surprisingly simple procedure.^{13,14} In this process, titanium dioxide (either with anatase or rutile structure), after treatment with a strong base followed by treatment with acid, readily gave tubular materials. The diameter of the resulting nanotubes was found to be 5–10 nm while the length of the tubes varied from 10 nanometers to many microns. Different commercial sources of titania powder^{15–17} as well as sol-gel synthesized titania¹⁸ all gave tubular titania type materials with similar nanotube structure. The temperature used for the base treatment was found to affect the shape of the titanium oxide nanostructure. Nano ribbon,¹⁹ nano belt,²⁰ nano fibre²¹ and nano whisker²² type structures could be synthesized by varying the synthesis conditions.

The nano titania produced by the electrochemical and template methods, gave amorphous titania while titania nanotubes produced by 'soft' chemical processes gave materials with good crystallinity. Initially it was believed that the tubular material had the anatase structure.^{13,14,16,21} Indeed XRD and Raman studies confirmed that the powder, after drying, consisted mainly of the

anatase phase. However, more recent studies^{1,16,20} have shown that the nanotubes are built from a layered titanate structure, with a structure of $\text{Na}_2\text{Ti}_2\text{O}_4(\text{OH})_2$ proposed for the nanotubes prior to acid treatment.²³ Sun has also studied the thermal stability of the nanotubes, and found that the sodium titanate phase is more stable than the protonated titanate phase.²⁴ Using the base-induced method, large arrays and continuous films of nanotubes have also been synthesized.²⁵

The phase change from nanocrystal anatase to nanocrystal rutile is known to occur at high temperature^{26–28} but the phase change can be reversed from rutile to anatase if the crystals are small enough.²⁹ The calculated particle size on the phase boundary between nanocrystalline anatase and rutile is about 14 nm. This suggests that anatase can only change into rutile when the size of the nanocrystal is larger than 14 nm. Cassier reported that ammonia-treated mesoporous titania yielded rutile on heating of the amorphous mesoporous titania at a temperature of 200°C and that the material changed into anatase at a temperature of between 300 and 350°C³⁰. For titania nanotubes, the reverse phase change for titania, from anatase to rutile, starts at a temperature of 700°C.¹⁸

Chen *et al.* proposed a tube formation mechanism in which the nanotube structure has a closed or scroll structure based on a layered trititanate.³¹ Wang *et al.*, from their study on nanotubes produced from NaOH, proposed a similar nanotube formation mechanism.³² In both proposals, a two-dimensional lamellar titanate was first formed in the strong base solution and this planar structure bent and finally rolled to form the tubular structure.

Two different kinds of layered structures of titanate, starting from either NaOH or KOH, have been observed.³³ However, limited information is available on these structures. In this contribution, Raman spectroscopy has been used to study the thermal stability of the titanate nanotube structures produced from both NaOH and KOH.

* To whom correspondence should be addressed. Fax: +27-11-7176749; Tel: +27-11-7176738; E-mail: ncoville@aurum.wits.ac.za

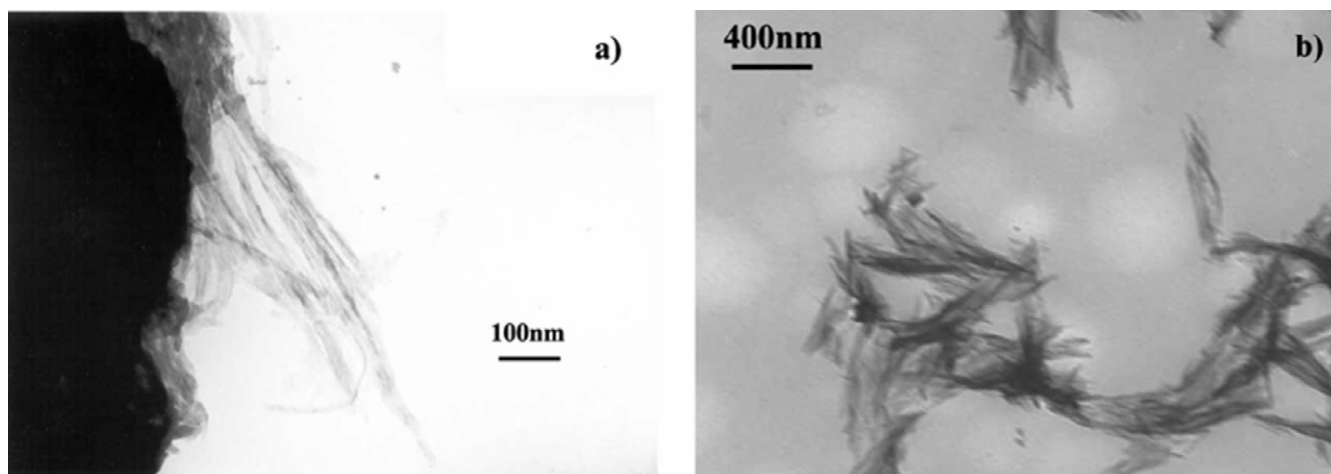


Figure 1 TEM pictures of samples (a) after base treatment, and (b) during washing.

2. Experimental

Titanate nanotubes were generated as described in the literature.¹³ Commercial titania powder (5 g, Degussa P25), a mixture of anatase and rutile phases, was added to either a NaOH or KOH aqueous solution (120 mL; 10M) and the mixture was then refluxed for 24 hours. The mixture was then diluted with distilled water and centrifuged at 10 000 rpm for *ca.* 20 minutes at 4°C. The material was allowed to settle and the water was decanted from the solid. The procedure was repeated until the conductivity of the supernatant reached 100 $\mu\text{S cm}^{-1}$. Samples were collected after different stages of the centrifugation process.

A HNO_3 (100 mL, 0.1 M) aqueous solution was then added to the solid product and the mixture was stirred at room temperature for 2 hours. The mixture was repeatedly centrifuged and washed with distilled water and then deionized water until the conductivity of the supernatant reached 10 $\mu\text{S cm}^{-1}$. Samples were also collected after different washing stages. The material was dried at room temperature under vacuum or at 120°C for 12 hours and calcined at 200°C, 300°C, 500°C and 1000°C for 4 hours in air. Samples were collected before and after the acid treatment, dried at room temperature under vacuum, and then characterized as a function of temperature in an *in situ* Raman study.

Raman analysis was carried out on a J-Y T64000 spectrometer. The *in situ* Raman study was carried out under argon at a heating rate of 5°C min^{-1} .

The morphology of the samples was evaluated using transmission electronic microscopy (TEM, JEOL 100S) and high-resolution transmission electronic microscopy (HRTEM, JEOL 2010). Samples for HRTEM analysis were prepared by sonicating about 1 mg material into 1 mL ethanol for 10 minutes and a few drops of the suspension was added to a hollow Cu grid coated with a carbon film (made in the laboratory or purchased from Ted Pella Inc., USA).

3. Results and Discussion

3.1. Effect of Washing after NaOH Treatment

The titanate nanotubes prepared by treatment of TiO_2 with NaOH were washed with water and the washing process was monitored by TEM and Raman spectroscopy to evaluate the effect of washing on the tube properties.

Figure 1 shows TEM pictures of the TiO_2 sample after NaOH treatment, and after washing and centrifugation. The pictures clearly reveal that the tubular structure of the sample was

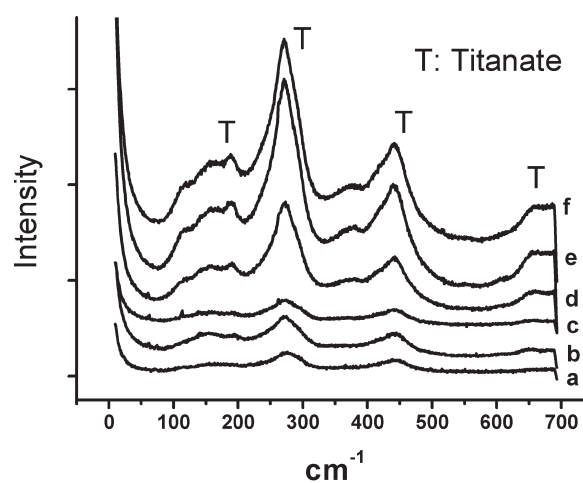


Figure 2 Raman spectra of titanate samples after base treatment (different washing stages). Conductivity of the supernatant ($\mu\text{S cm}^{-1}$): a) 19 000; b) 4500; c) 410; d) 230; e) 180; f) 81.

already formed in the initial strong base solution. Fig. 2 shows the Raman spectra of various NaOH-treated samples with their corresponding conductivity values. In all the spectra, peaks are seen at 188, 271, 441 and 652 cm^{-1} . These peaks (labelled T) correspond to a titanate species and the Raman spectrum is similar to that described in Ref. 14 (Fig. 4, Sample B) prior to acid addition. EDX analysis of the materials was also carried out and revealed that even after the titanate nanotubes has been washed and centrifuged till the conductivity of supernatant was lower than 100 $\mu\text{S cm}^{-1}$, a large amount of sodium ions (17%) was left in the sample. This suggests that the structure of the tubes corresponds to a sodium titanate material. It is to be noted that the intensities of the Raman peaks increased with washing, indicating that the crystallization of the sodium titanate nanotubes (or purity) improved during the washing process.

3.2. Effect of Aging of the NaOH-treated TiO_2 .

The effect of aging time on the formation of the sodium titanate nanotubes was studied. After the base treatment, the sample was kept in the strong base solution for different times (1–225 days) before the washing procedure. The sample aged for one day shows that almost all the material observed had a tubular structure. Less tubular structures were found in the samples analysed after long aging times, i.e. the longer the solid was kept in the base solution, the less the amount of tubular structure

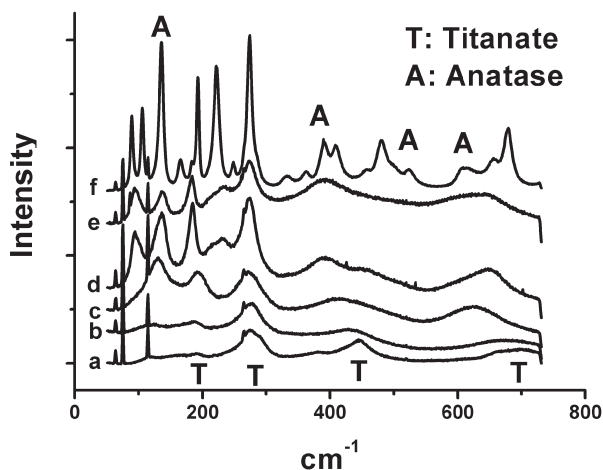


Figure 3 *In situ* Raman of spectra sodium titanate nanotubes (temperature in °C): a) 27; b) 700; c) 800; d) 900; e) 1000; f) cooled to 27.

found in the final products after washing. A Raman study of the aged samples (225 days) showed that after the long aging time that the material still corresponded to sodium titanate. This study indicates that the tubular structure is not stable in strong base solution. The tubular titanate structures slowly changed into a bulk amorphous titanate structure in the strong base solution.

3.3. *In situ* Raman Study of the Effect of Temperature on Sodium Titanate Nanotubes

An *in situ* Raman study of the effect of temperature on sodium titanate nanotubes is shown in Fig. 3. As found by Sun and Li,²⁴ we also observed that the sodium titanate is stable at high temperature. In Fig. 3a, peaks were observed at 190, 270, 440, 690 cm^{-1} and correspond to a titanate structure.¹⁴ This structure was stable up to 700°C (Fig. 3b). As shown in Fig. 3c, at high temperature ($T = 800^\circ\text{C}$), a peak appeared at 130 cm^{-1} , and the peaks at 440 and 690 cm^{-1} shifted to lower wave numbers, indicating a new phase had formed. Spectra become more complicated at higher temperatures, as shown in Fig. 3d (900°C) and 3e (1000°C). The peak at 130 cm^{-1} shifted slightly to 133 cm^{-1} , while two new peaks were observed at 95 cm^{-1} and 230 cm^{-1} . On cooling from 1000°C to 27°C new peaks appeared (Fig. 3f), indicating that new phases had formed. It is not clear as to what phases had formed after the sample was heated above 700°C, while after cooling some anatase was detected (Fig. 3f).

3.4. Acid Treatment

Figure 4a shows the Raman spectra of the titanate nanotubes (produced from NaOH) after acid treatment, washing by centrifugation, and drying under vacuum. The spectra show that the titanate structure is retained after acid treatment. Figure 5 shows the HRTEM of titanate nanotubes after the acid treatment and washing with water and drying at 120°C. EDX analysis of the sample reveals that there are only trace amounts of sodium (0.3%, close to the detection limit) left in the material. The HRTEM and EDX data suggest that protonated titanate nanotubes have been produced.

The walls of the protonated nanotubes show that the distance between two titanate layers in the [001] direction is 0.51 nm. This is shorter than that of protonated titanate structures listed in the literature.³³ It has been reported that the layer distance between two titanate layers in the [001] direction could be reduced upon heating.³³ This may explain the short layer distance observed in our study. At the tube end, a layer distance of 0.38 nm was

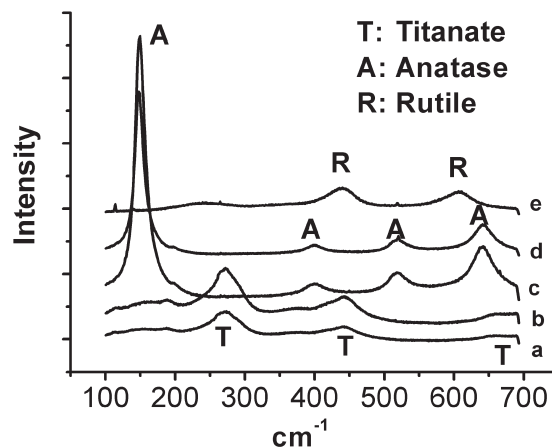


Figure 4 Raman spectra of protonated titanate samples after acid treatment and dried/calced at (temperature in °C): a) room temperature; b) 200; c) 300; d) 500; e) 1000; and for 4 hours in air.

observed, which is the layer distance of protonated titanate in the [010] direction.

3.5. *In situ* Raman of the Protonated Titanate Nanotubes Produced from NaOH

An *in situ* Raman study of protonated titanate nanotubes (produced from NaOH) as a function of temperature is shown in Fig. 6. The protonated titanate structure, as indicated by peaks at 275 and 449 cm^{-1} (labelled T), was stable up to 150°C. Anatase peaks (153, 206, 391, 505 and 615 cm^{-1}) appeared when the temperature reached 300°C.¹⁴ It is interesting to note that in the temperature range between 150°C and 300°C, the sample interacted with the laser beam, as detected by sample darkening at the position of laser–titanate interaction site. This was not observed at a lower or higher temperature. A weaker laser power of 20 mW was applied to avoid the ‘burning’ phenomenon detected when 50 mW power was used. No significant Raman peaks were found in the temperature range of 150 to 300°C. This darkening effect suggests that during the phase change, the

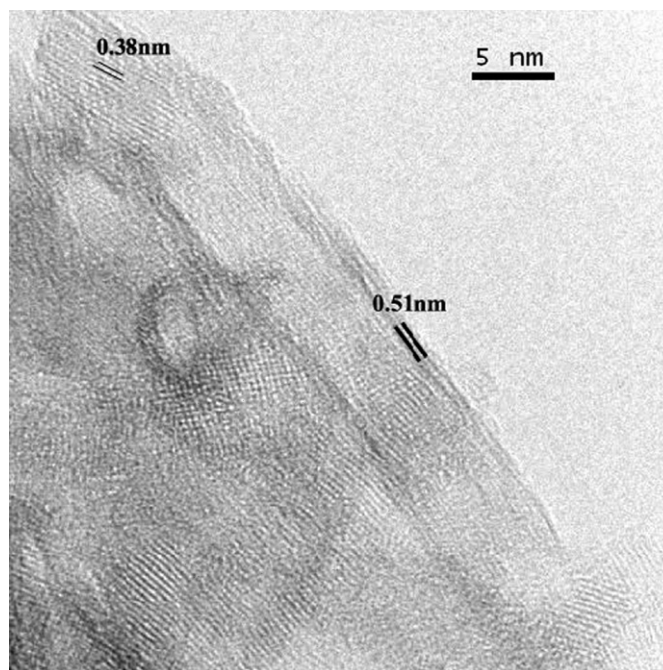


Figure 5 HRTEM of titanate nanotubes (after acid treatment, formed from NaOH) dried at 120°C in air.

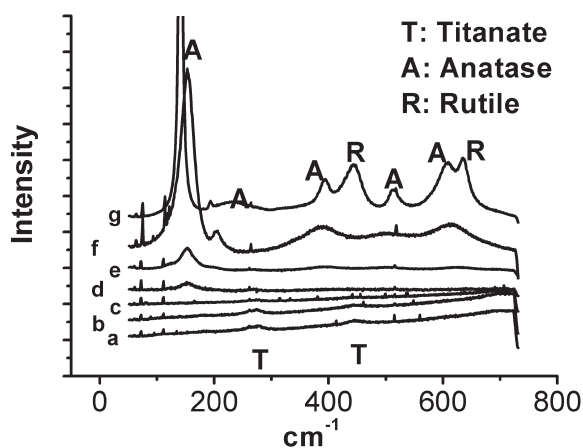


Figure 6 *In situ* Raman spectra of protonated titanate samples prepared from NaOH at (temperature in °C): a) 25; b) 120; c) 150; d) 300; e) 600; f) 1000; g) cooling from 1000 to 27.

amorphous material is very photosensitive.

The conversion of protonated titanate to anatase was complete at 300°C. Thereafter the intensities of the anatase peaks become more obvious with an increase in temperature. The sample was kept at 1000°C for 10 minutes. The Raman spectrum indicates that the sample is still predominantly anatase, although the main peak shifts to a lower wave number (153 cm^{-1}). This could be caused by an oxygen deficiency taking place during heating under argon³⁴. After cooling from 1000°C to room temperature, the main Raman peak of anatase shifted to 141 cm^{-1} . It is interesting to note that the presence of some rutile material¹⁴

(peaks at $442, 635\text{ cm}^{-1}$) was observed in the spectrum after sample cooling (Fig. 6g). This suggests that the phase change from anatase to rutile is a slow process when the anatase is prepared from sodium titanate nanotubes.

Figure 7 shows the TEM pictures of samples analysed after the acid treatment, (washed and dried), and calcined at different temperatures. The data shows that the tubular structure was the dominant structure even after sample calcination at 500°C for 4 hours. Raman spectra (Fig. 4b–4e) of the samples showed that when the sample was calcined at a temperature of 200°C (Fig. 4b), the protonated titanate structure was maintained. When a calcination temperature $>200^\circ\text{C}$ was used, the tubular structure was maintained and the protonated titanate changed into anatase. Many tubular structures were broken in the process (Fig. 7c). At a calcination temperature of 1000°C, only the rutile phase was observed in the Raman spectra (Fig. 4e) and no tubular structure was detected (Fig. 7d).

Comparison of the results of the *in situ* Raman study of the sodium titanate nanotubes and protonated nanotubes revealed that the sodium titanate tubes are more stable than the protonated nanotubes. It is assumed that the sodium ion fits inside the titanate layer, and hence the structure of sodium titanate was more thermodynamically stable than that of the protonated titanate.

3.6. *In situ* Raman of Protonated Titanate Nanotubes Produced from KOH

An *in situ* Raman study of the protonated titanate nanotubes produced from KOH as a function of temperature is shown in Fig. 8. The study was similar to that of the protonated titanate

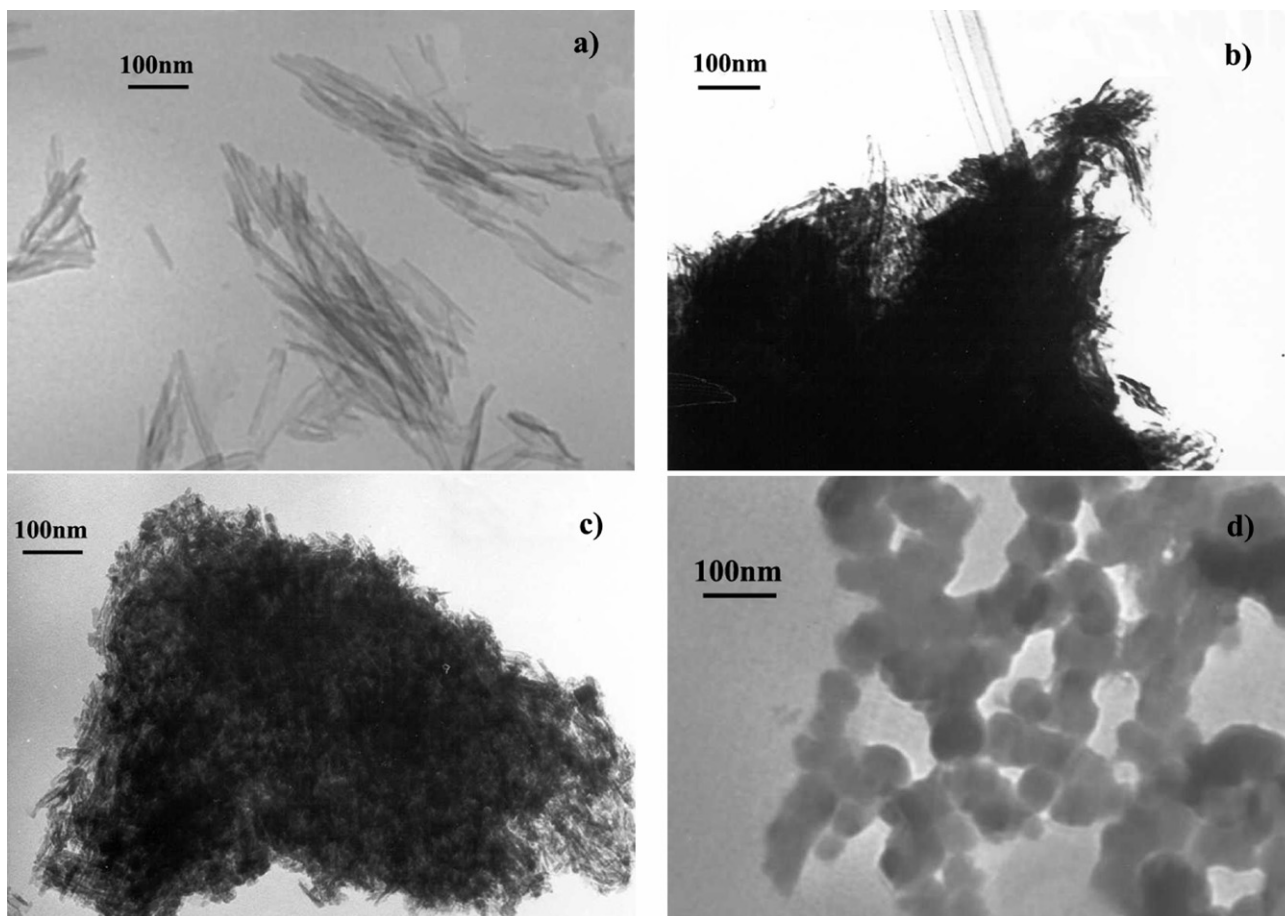


Figure 7 TEM morphology of titanate samples after acid treatment: (a) dried at room temperature; (b) dried at 120°C for 12 hours; (c) calcined at 500°C for 4 hours; (d) calcined at 1000°C for 4 hours in air.

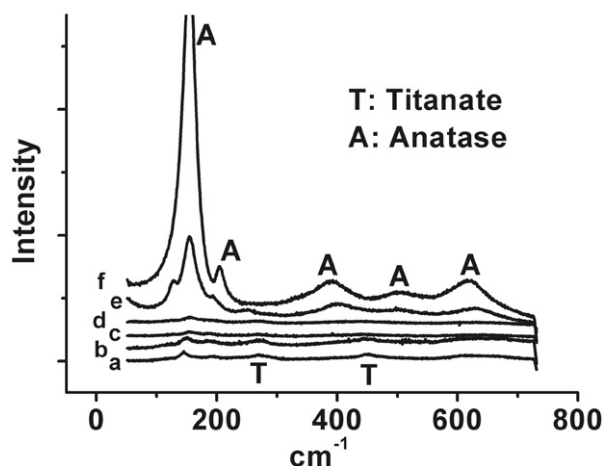


Figure 8 *In situ* Raman spectra of protonated titanate samples prepared from KOH at (temperature in °C): a) 25; b) 120; c) 150; d) 300; e) 600; f) 1000.

nanotubes prepared from NaOH. TEM studies (not shown) show that the shape and size of the nanotubes prepared from NaOH and KOH are the same. The initial phase detected for the material prepared from KOH was protonated titanate (peaks at 275 and 449 cm^{-1} , Fig. 8a). These peaks became weaker on heating and eventually disappeared at a temperature of 150°C. The phase change was complete at $T < 300^\circ\text{C}$, the same temperature at which the protonated titanate from NaOH was converted to anatase. For $T > 300^\circ\text{C}$, the anatase peaks (153, 206, 391, 505 and 615 cm^{-1}) became more intense on heating. No rutile peaks were detected at 1000°C, even after 10 minutes. This is to be compared with the formation of the rutile phase produced from the sample produced from NaOH.

The study thus reveals that the phase change of the protonated titanate nanotubes is from titanate to anatase, and is independent of the base source used.

Protonated titanates produced from either NaOH or KOH have different structures in the bulk phase (Fig. 9).³³ In the bulk phase, the protonated titanate from a sodium source has an AAA

structure while the protonated titanate from a potassium source has an ABA structure.

During heating, the layer distance becomes shorter and eventually close enough to initiate the phase change. In the case of the AAA structure, titanate could change into anatase directly, while in the case of the ABA structure, a beta-titanium phase is first formed from protonated titanate, which then changes into anatase on further heating. The *in situ* Raman study of the protonated titanate nanotubes from both sodium and potassium sources show that the phase changes are the same in both cases, i.e. the protonated titanate changes directly into anatase. This suggests that when the tubular structure is formed, especially in the case of nanotubes prepared from the potassium source, no multiple layer structure of the bulk titanate was involved. In other words, when the titanate sheet rolled into the tube, the sheet was only one layer thick. This may explain why reaction of titania with potassium hydroxide gives a wider range of structures – ribbons,¹⁹ belts,²⁰ fibres²¹ and whiskers²² – rather than tubes. Once a multiple layer structure of potassium titanate is formed, the tubular structure will be difficult to synthesize.

4. Conclusion

This study reveals that the treatment of titania with strong base gives tubular titanate species and that the tubular structures are prepared prior to washing and are independent of base type (KOH, NaOH). Calcination of the tubular material (NaOH) generates a new material that still needs to be evaluated. Treatment of the Na or K containing titanate with acid results in removal of the Na^+ and K^+ ions but with retention of the tubular structure. Upon calcination the protonated titanate converts to anatase TiO_2 with little formation of rutile TiO_2 , even at high temperature ($>800^\circ\text{C}$), especially if NaOH is used as base.

Acknowledgements

We thank Dr Rudolf Erasmus from University of Witwatersrand for recording the Raman spectra, Dr Huifang Xu from the University of New Mexico for the HRTEM results and the University of the Witwatersrand, the NRF and THRIP for financial support.

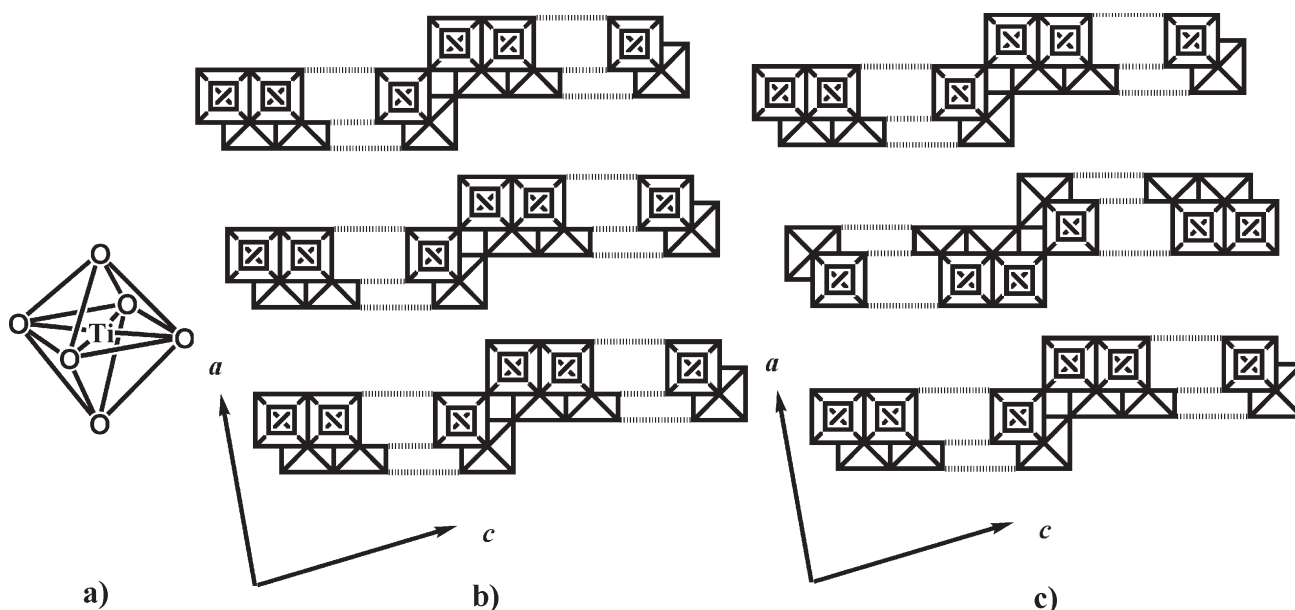


Figure 9 The structure of bulk titanate: (a) the octahedral structure of TiO_6 is represented by a square in (b) and (c); (b) the AAA structure of protonated titanate prepared from a sodium source; (c) the ABA structure of protonated titanate prepared from a potassium source. The square with a small square inside represents the TiO_6 octahedron in a top layer while the half square without an internal square represents the TiO_6 octahedron in a lower layer.

References

- 1 G.P. Patzke, F. Krumeich and R. Nesper, *Angew. Chem. Int. Ed.*, 2002, **41**, 2446.
- 2 O.K. Varghese, D. Gong, M. Paulose, K.G. Ong and C.A. Grimes, *Sensors and Actuators B*, 2003, **93**, 338.
- 3 C.A. Grimes, K.G. Ong, O.K. Varghese, X. Yang, M. Paulose, E.C. Dickey, C. Ruan, M.V. Pishko, J.W. Kendig and A.J. Mason, *Sensors*, 2003, **3**(3), 69.
- 4 S. Uchida, R. Chiba, M. Tomiha, N. Masaki and M. Shirai, *Studies in Surface Science and Catalysis*, 2003, **146**, 791.
- 5 M. Adachi, Y. Murata, I. Okada and S. Yoshikawa, *J. Electrochemical Soc.* 2003, **150**(8), G488.
- 6 P. Hoyer, *Langmuir* 1996, **12**, 1411.
- 7 H. Imai, Y. Takei, K. Shimizu, M. Matsuda and H. Hirahima, *J. Mater. Chem.* 1999, **9**, 2971.
- 8 M. Zhang, Y. Bando and K. Wada, *J. Mater. Sci. Lett.* 2001, **20**, 167.
- 9 S. Kobayashi, K. Hanabusa, N. Hamasaki, M. Kimura and H. Shirai, *Chem. Mater.* 2000, **12**, 1523.
- 10 J.H. Jung, H. Kobayashi, K.J.C. van Bommel, S. Shinkai and T. Shimizu, *Chem. Mater.* 2002, **14**, 1445.
- 11 R.A. Caruso, J.H. Schattka and A. Greiner, *Adv. Mater.* 2001, **13**, 1577.
- 12 D. Gong, C.A. Grimes, O.K. Varghese, W. Hu, R.S. Singh, Z. Chen and E.C. Dickey, *J. Mater. Res.* 2001, **16**, 3331.
- 13 T. Kasuga, M. Hiramatsu, A. Hoson, T. Sekino and K. Niihara, *Langmuir*, 1998, **14**, 3160.
- 14 T. Kasuga, M. Hiramatsu, A. Hoson, T. Sekino and K. Niihara, *Adv. Mater.*, 1999, **11**, 1307.
- 15 G.H. Du, Q. Chen, R.C. Che, Z.Y. Yuan and L-M. Peng, *Appl. Phys. Lett.*, 2001, **79**, 3702.
- 16 C-H. Lin, S-H. Chien, J-H. Chao, C-Y. Sheu, Y-C. Cheng, Y-J. Huang and C-H. Tsai, *Catal. Lett.*, 2002, **80**, 153.
- 17 Q. Zhang, L. Gao, J. Sun and S. Zheng, *Chem. Lett.*, 2002, 226.
- 18 D-S. Seo, J-K. Lee and H. Kim, *J. Crystal Growth*, 2001, **229**, 428.
- 19 Z-Y. Yuan, J-F. Colomer and B-L. Su, *Chem. Phys. Lett.*, 2002, **363**, 362.
- 20 X. Sun, X. Chen and Y. Li, *Inorg. Chem.*, 2002, **41**, 4996.
- 21 Z-Y. Yuan, W. Zhou and B-L. Su, *Chem. Comm.*, 2002, 1202.
- 22 Y. Zhu, H. Li, Y. Koltypin, Y.R. Hacoheh and A. Gedanken, *Chem. Comm.*, 2001, 2616.
- 23 J. Yang, Z. Jin, X. Wang, W. Li, J. Zhang, and S. Zhang, *Dalton Trans.*, 2003, 3898.
- 24 X. Sun and Y. Li, *Chem. Eur. J.* 2003, **9**, 2229.
- 25 Z.R. Tian, J.A. Voigt, J. Liu, B. McKenzie and H. Xu, *J. Am. Chem. Soc.*, 2003, **125**, 12384.
- 26 A.A. Gribb and J.F. Banfield, *Am. Miner.*, 1997, **82**, 717.
- 27 H. Zhang and J.F. Banfield, *Am. Miner.*, 1999, **84**, 528.
- 28 R.L. Penn and J.F. Banfield, *Am. Miner.*, 1999, **84**, 871.
- 29 H. Zhang and J.F. Banfield, *J. Mater. Chem.*, 1998, **8**, 2073.
- 30 K. Cassiers, T. Linssen, V. Meynen, P. Van Der Voort, P. Cool and E.F. Vansant, *Chem. Comm.*, 2003, 1178.
- 31 Q. Chen, G.H. Du, S. Zhang and L-M. Peng, *Acta Cryst.*, 2002, **B58**, 587.
- 32 Y.Q. Wang, G.Q. Hu, X. F. Duan, H.L. Sun and Q.K. Xue, *Chem. Phys. Lett.*, 2002, **365**, 427.
- 33 T. Sasaki, Y. Komatsu and Y. Fujiki, *Chem. Mater.*, 1992, **4**(4), 896.
- 34 H. Liu, W. Yang, Y. Ma, Y. Cao, J. Yao, J. Zhang, and T. Hu, *Langmuir*, 2003, **19**, 3001.